HEIMDAL - FIRST SCIENCE

(FIRST DRAFT 04/26)

	Name	Role/Title
Owner	Dan Mannix	HEIMDAL – Lead instrument scientist
Reviewer		
Approver	Mikhail Feygenson	Head of Diffraction and Imaging Division

1. INTRODUCTION

1.1. Purpose of this document

This document outlines the plan for the first science at the HEIMDAL instrument. It is a living document that will be revised up to the start of hot commissioning. The first draft includes science input from the Heimdal in-kind partners, ESS, IFE, AU and PSI and associated national science groups. The ideas are currently being expanded towards a first science workshop at the ESS/ILL user meeting. Beamtime should also be considered for the eventual second scientist of Heimdal that will be hired later in 2026.

Chapter 2 gives the expected timing for Heimdal hot commissioning and first science. Chapter 3, give the instrument technical specifications, that can be used to devise feasible experiments. Chapter 4 overviews the hot commissioning and first science plan, including suggestions for known samples and bench marking experiments and input for actual first science ideas.

2. INTRODUCTION

Heimdal is neutron diffraction instrument located on port W8 of the ESS. The full scope concept of the instrument combines neutron diffraction, SANS and imaging to provide a multi-length-scale analysis of advanced materials from 10^{-11}-10^{-2}m. Due to financial limitations, the initial scope of the instrument focuses on diffraction, with SANS and imaging forming later upgrades. For the purpose of the discussion of first science this document will focus on the diffraction science potential of Heimdal. Heimdal is equipped with a motorised x,y,z and omega sample stage, which will enable both powder and single crystal diffraction techniques on samples down to 1mm in size. Heimdal is designed to be a multipurpose neutron diffraction instrument for advanced materials science research. The original science case was targeted at the following materials:

(1) Light elements and energy related materials
(2) Composites, scaffolds or matrix embedded systems
(3) Phase transition and nucleation
(4) Materials with magnetic properties.

The first science activities will finalise the hot commissioning phase of the instrument, before the start of user operations phase and is designed to benchmark or showcase the capabilities of the instrument. The hot commissioning plan is divided into the 4 sections.

Phase 1: Component validation with neutrons

Phase 2: Instrument calibration

Phase 3: Standard samples and benchmarking

Phase 4: Early Science experiments.

Phase 1, will commission certain components such as the monitors, the chopper cascade and phasing and uniformity of the detector. Phase 2, calibrate the instrument using standard samples to enable

the connect conversion from TOF to real spacing. Phase 3 will test the instrument on well known example samples as a proof of principle of the instrument concept and software and can be used to bench mark the instrument in terms of diffraction intensities and resolution. Phase 4, will be used for real case experiments on unknown to possible previously characterised systems. It is expected that external user groups will contribute to phase 3&4 of hot commissioning. The Heimdal hot commissioning phase is currently scheduled for mid 2027 and the timing with the current expected ESS accelerator power is shown in **figure 1**. Optimistically, during the first science activities, we can expect the flux to be around 5-10% on the 2MW total flux provided when the accelerator is operated at full power. At this point the flux of Heimdal should be comparable to other diffraction neutron instruments such as WISH, but with possibility for high wave-vector resolution.

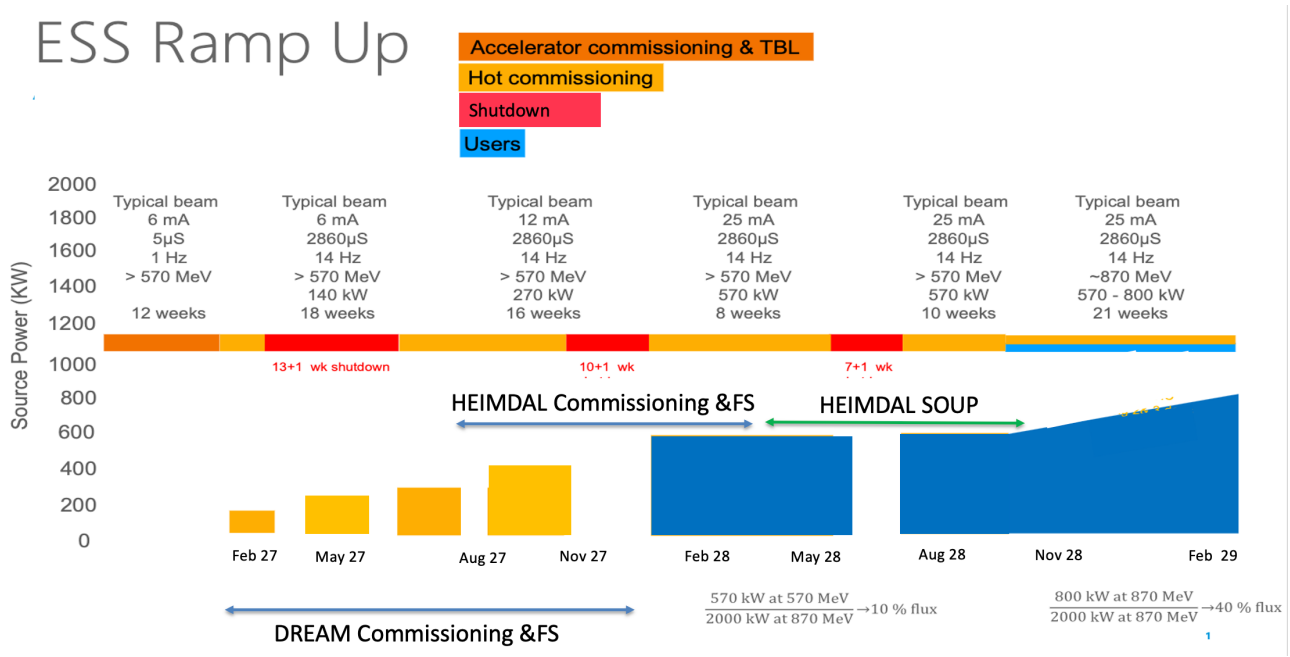

Figure 1. The expected accelerator power and timing of Heimdal hot commissioning, to be confirmed.

3. HEIMDAL SPECIFICATIONS

Here, we give an overview of the technical specification of the Heimdal instrument, which is aimed at helping groups to check the feasibility of first science experiments.

3.1. Heimdal Components & Locations

The thermal guide of the Heimdal instrument views both the thermal and cold moderators of the ESS and is bi-spectral. Cold neutrons can be deviated into the thermal guide using a bi-spectral switch located inside the BBG. The Heimdal thermal guide is designed to transport neutrons in the wavelength range of 0.6-6Å with a natural bandwidth of 1.7Å and with a divergence of ±0.5˚ into a spotsize of 20mm(V)x5(H)mm. The divergence can be tuned to match the instrument resolution by using a set of three divergence slits. The main instrument components together with their distances from the source are shown in **figure 2.**

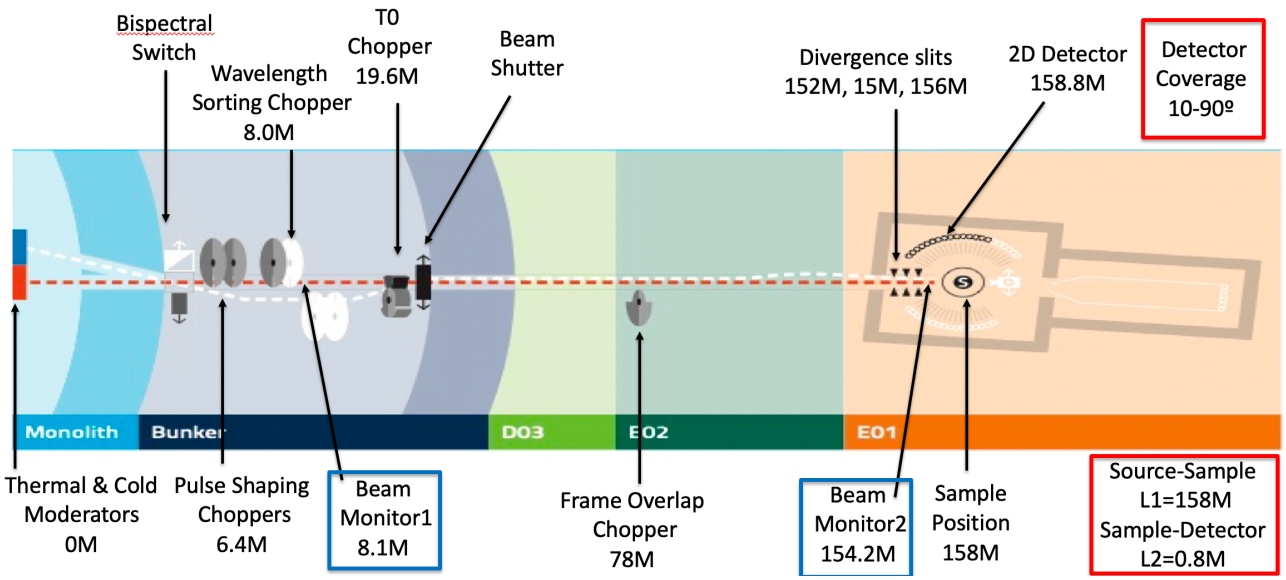

Figure 2. The components and positions of Heimdal components relate to the neutron source.

3.2. Heimdal Detector Specifications

Heimdal will employ a CDT Jalousie type 2D (3D) detector based on ^{10}B technology similar to Dream and Magic instruments at ESS. For the first science activities, the detector coverage is expected to be fixed to 10-90°, which will limit the accessible Q-range of the instrument. Work is on-going to rescope these detectors as soon as possible to extend the coverage to 10-170°, although it is unsure and unlikely at this time if this will be completed before the start of first science. The detector specifications and drawing are shown in **figure 3**.

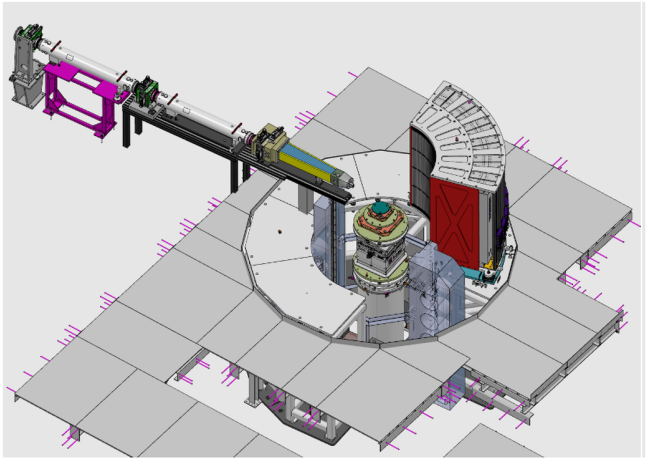

CDT ^{10}B Detectors (sample-detector distance = 0.8M)
2θ Horizontal Coverage: 10-90°
Δ2θ Horizontal Resolution: 1.03mm 0.08° FWHM
Φ Vertical Coverage: ±22.0°
ΔΦ Vertical Resolution: 6.7mm 0.53° FWHM
Pixel Size: 1.03x6.7mm (HxV)

Radial pixels size (**Δ**R) = 17.1mm
Time Resolution (**Δ**t) = 3µs

Detector Efficiency: 50% @0.8Å. 70% @3Å

Max Count rate ~500kHz (not tested)

Figure 3. A schematic of the Heimdal 2D detector and technical specifications.

3.3. Heimdal Flux and Resolution

The PSC frequency can be selected to completed tune the Heimdal wave-vector resolution from 10^{-2} – 10^{-4} with a similar trade off in incident flux. The flux and resolution for various chopper speeds (e.g. n=1=14Hz, n=10=140Hz etc.) is shown in figure 4.

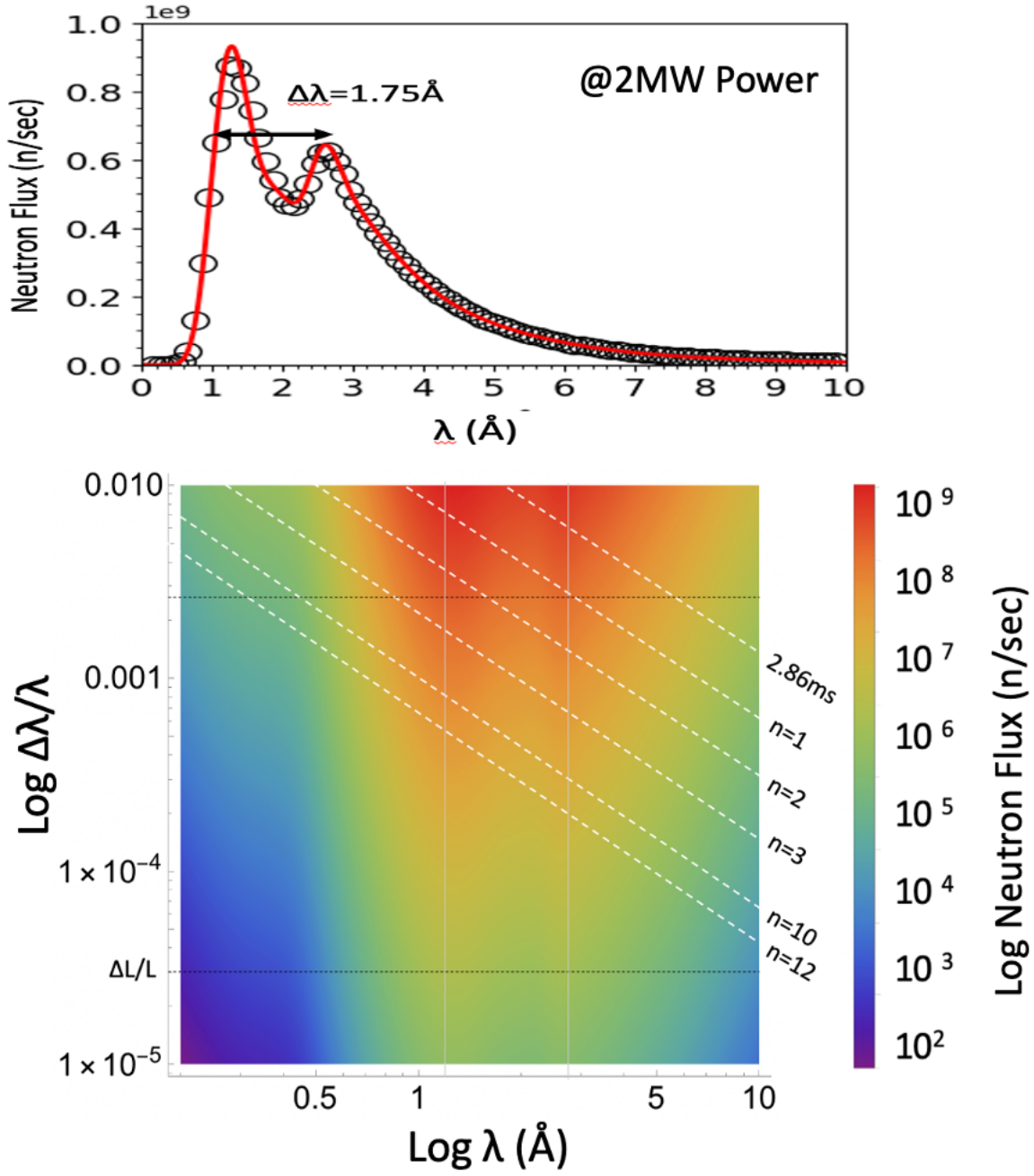

Figure 4. (Top) Flux vs wavelength for Heimdal at 2MW power (linear scale). (Bottom) Log resolution and log flux vs for various wavelengths for different chopper speeds (white dashed lines).

For the interest of discussing the wave-vectors accessible on Heimdal, for simplicity to describe four 1.7Å bandwidth scenarios across the most intense part of the Heimdal energy spectrum, for a fixed detector angle of 10-90° (see **table 1** below). These are a, thermal High-Q band from 0.6-2.3Å, using the lowest wavelength neutrons, a thermal/cold high flux band from 1.0-2.8Å across the highest flux region of the neutron energy spectrum, a cold band from 2-3.7Å entering the cold part of the neutron spectrum and a cold-lowQ band from 3.0-4.7Å of the cold regime with fairly high flux. The accessible Q-range for these bands, together with the average flux per band expected during first science (for 1% resolution) are shown in **table 1**.

Day-1 Scope Detectors (10-90 Degrees)										
Band type			Thermal High-Q		Thermal/Cold High Flux		Cold		Cold Low-Q	
Band Wavelength			λ = 0.6-2.3Å		λ = 1.0-2.8Å		λ = 2.0-3.7Å		λ = 3.0-4.7Å	
Detector Coverage	2θ Max	2θ Min	Q Max ($Å^{-1}$)	Q Min ($Å^{-1}$)	Q Max ($Å^{-1}$)	Q Min ($Å^{-1}$)	Q Max ($Å^{-1}$)	Q Min ($Å^{-1}$)	Q Max ($Å^{-1}$)	Q Min ($Å^{-1}$)
	90	10	14,809173	0,47617351	8,88550381	0,39114252	4,44275191	0,29599975	2,9618346	0,23302108
Av. Flux for First Science (0.57MW)			$1.8x10^7$		$5.6x10^7$		$4.3x10^7$		$2.1x10^7$	

Table 1. Four wavelength bands with the accessible Q-range and average flux expected during first science activities on Heimdal.

3.4. Heimdal Sample Environment

Heimdal has a broad science case covering a diverse range of materials systems that will require the implementation of a broad range of sample environments to be adapted for the instrument. We rely extensively on the sample environment pool for this hardware. Heimdal is designed to employ a collimator to supress the parasitic scattering from sample environments. Ideally we wish to hot commission all of the sample environments available in the hot commissioning and first science stage to assess their background levels and eventual experiment feasibility for user operations. Furthermore, Heimdal currently offers no vacuum chamber around the sample and the level of air scattering background together with background from sample environment will need to be assessed particular for powder neutron diffraction, due to the diffuse nature of powder scattering compared to single crystals. The sample environments under consideration are shown in table 2 below and in figure 5.

Sample Environment	Rating	Comments
Orange Cryostat	1	HC Background measurement required.
Dry Cryofurnace	1	HC Background measurement required
Wet He Cryofurnace	1	HC Background and test experiment required
Dilution Fridge	1	HC Background and test experiment required
Heat gun/cryojet sample changer	1	HC Background and test experiment required
Vanadium furnace	1	Background required
6.5T Cryomagnet	1	Background and test experiment
8.0T Cryomagnet	1	Background and test experiment required
Potentiostat (Electrochemistry)	2	Background required
Electrochemistry Cells	2	Background required
Small Stress rig	3	Feasibility study required before user experiment
Paris Edinburgh press	1/2	Background and test experiment required.
HP Cryostat	3	Feasibility study required before users experiments

Gas Pressure Cells	3	Feasibility study required before users experiments
Clamp Cells	3	Feasibility study required before users experiments
Liquid Pressure Cells	3	Feasibility study required before users experiments
DAC	3	Feasibility study required before users experiments

Table 2. Various sample environment available from the sample environment group.

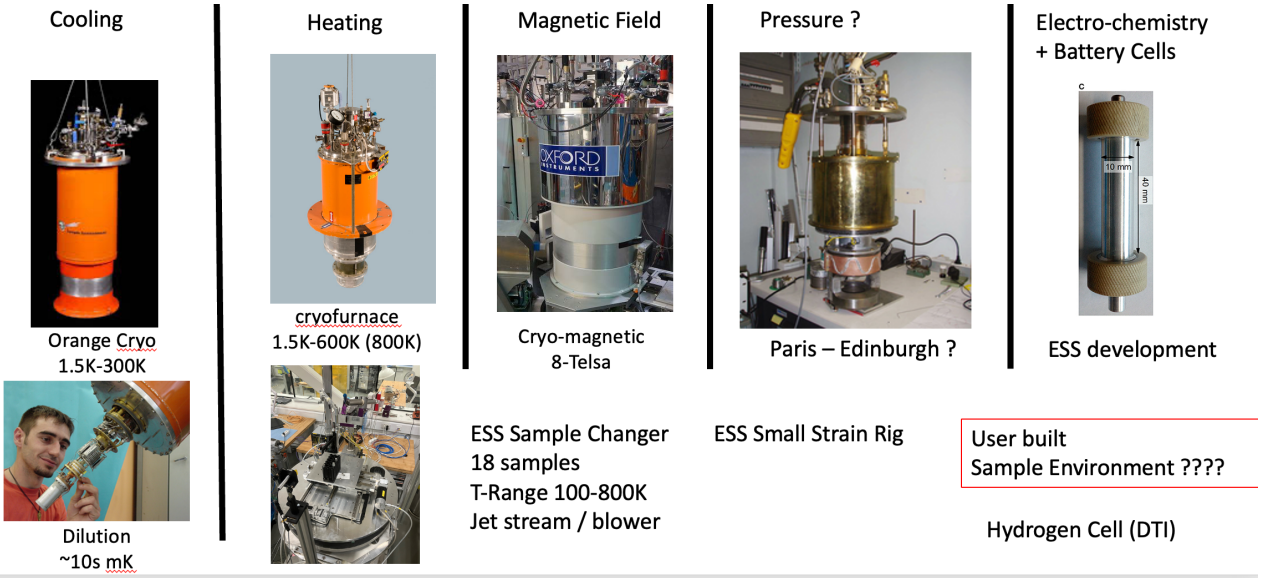

Figure 5. Various sample environments to be tested during hot commissioning and first science on Heimdal.

4. HOT COMMISSIONING & FIRST SCIENCE PLAN

4.1. Phase 1: Component validation with neutrons

Phase 1 will consists of validation of various components similar to other instruments at ESS and these activities are beyond the scope of this first science document.

4.2. Phase 2: Instrument calibration

Here we plan to use the same powder and single crystal standards to Dream to calibrate the instrument and to compare flux and resolutions of the two instruments. Examples of these standards are shown in table 3 below.

Standard Sample	Form	TEST
Si (NIST SRM640f)	Powder standard	Calibration line position and instrument response
LaB_6	Powder standard	Calibration line shape

Al_2O_3	Powder standard	Calibration peak positions
$Y_3Fe_5O_{12}$ (YIG)	Powder standard	Calibration magnetic
Mica (SRM 675)	Powder standard	Calibration large d-spacing
Silver behenate $AgC_{22}D_{43}O_2$	Powder standard	Calibration large d-spacings
$Y_3Fe_5O_{12}$ (YIG)	Powder standard (magnetic)	Calibration magnetic

Table 3. Examples of standard powder samples to be used for calibration of Heimdal.

Examples of single crystals to be used for calibration experiments are given in table 4 below.

Standard Sample	Form	TEST
Si High purity	Single Crystal of various sizes 1-5mm.	Calibration peaks position and instrument response size vs scattering / time to collect data using Laue TOF.
Al_2O_3	Single Crystal	Calibration line shape
$Y_3Fe_5O_{12}$ (YIG)	Single Crystal	Calibration peak positions
NiO	Single Crystal	Calibration antiferromagnetic Bragg peaks

Table 4. Examples of single crystals to calibrate Heimdal.

4.3. Phase 3: Standard samples and benchmarking

Here, the objectives are to test the Heimdal instrument with well known and studied results to verify that the instrument can reproduce similar results. These results can also be used to bench mark the instrument with respect to other neutron instruments at other facilities. This work will also involve as far as possible and as widely as possible the diverse sample environments to characterise the background from sample environment and air scattering in order to assess any potential issues for start of user operations. In table 5 below, we summarise a list of potential standard samples for hot commissioning, with a brief discussion afterwards.

Experiment	Sample	Sample Environment	Comments
Simple AFM structures	NiO / MnO powders	Cryostat	Well known magnetic and simple FCC structural refinement
Incommensurate charge/spin waves	Chromium single crystal & powder	Cryostat	Well known sample test of incommensurate structure diffraction. Weak SDW powder peaks vs background

Holmium magnetic scattering	Large single crystal	Cryostat	Refinement of spiral magnetic structure. Spin slip structures (high resolution)
Spin density wave	TmNi2B2C single crystal	Dilution	SDW forms below Tn=1.5K. Test of dilution cryostat.
Spin Seebeck Effect materials	$Tb_3Fe_5O_{12}$ Powder/SC	Cryofurnace 2-600K	Magnetic structure changes across broad temperature range. High resolution. Background.
Very low temperature + Field	$Tb_3Ga_5O_{12}$ single crystal	Dilution + 6T magnetic field	Magnetic Order below 250mK applied field changes structure. Tests of dilution + magnetic field.
Magnetic thin films	BiFeO3 100nm TbIG 100nm	Cryostat	Test of High flux, low background, good resolution. Feasibility study for thin films
Time Resolved reduction experiments Mogens Christensen	Fe2O3 in H2. Fe3O4	Furnace + H2	Test of low resolution, high flux mode and time resolved diffraction. Test of furnace and H2 environments.

Table 5. List of potential standard samples for benchmarking and sample environment tests.

4.3.1.MnO and NiO simple antiferromagnets

MnO was used for the first demonstration of neutron magnetic scattering from an antiferromagnet compound by Shull and co-worker. Both NiO and MnO are simple FCC structures and show similar magnetic structures described by ferromagnetic (111) planes stacked antiferromagnetically to give a magnetic propagation vector of Q_m=(½ ½ ½). The simple chemical and magnetic structures should be an easy refinement test for the instruments.

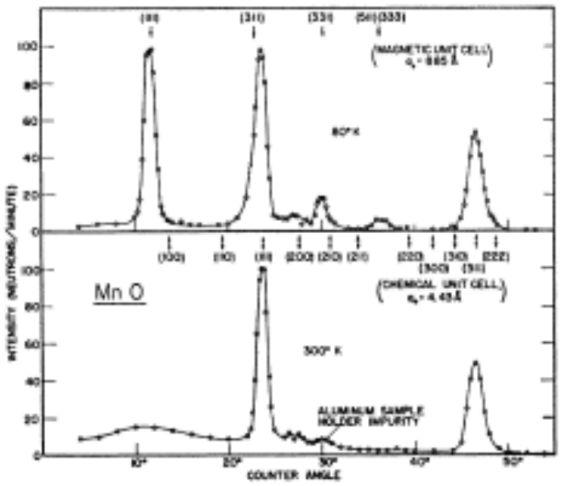

FIG. 1. Neutron diffraction patterns for MnO at room temperature and at 80°K.

C. G. Shull & J. S. Smart, Phys. Rev. **76** (1949) 1256

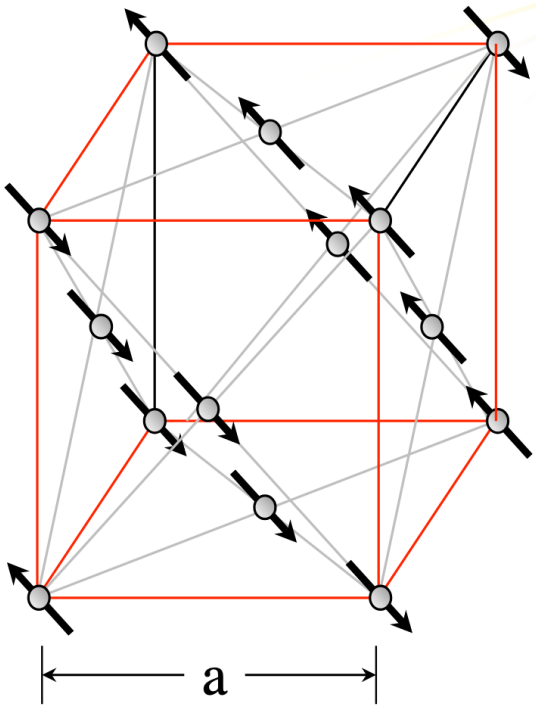

Figure 6. (Left) Neutron diffraction from MnO showing the onset of AFM peaks. (Right) The magnetic structure of MnO.

4.3.2. Chromium Metal

Chromium is a famous magnetic material forming both incommensurate spin density wave SDW) and charge density wave (CDW) structures by fermi surface nesting below T_N=311K. The SDW and CDW have been studied widely using both neutron and x-ray magnetic scattering techniques, making an excelled benchmarking system for HEIMDAL The magnetic moment of the SDW is relatively small with 0.6μ_B. The experiment will attempt to resolve the Bragg peak satellites from the SDW using both powder and single crystal diffraction. An example of the scattering around the (2 0 0) Structural Bragg peak is shown in the figure below. The date were taken with high wavevector resolution of $\Delta\lambda/\lambda \sim 10^{-3}$. This makes an interesting test case for tuning flux and resolution of HEIMDAL to resolve these peaks. The experiment will also provide some good benchmarking of the dynamical range and background limitation of the new detector CDT Jaolasie detector technology The SDW phase maybe modified in nanoscale powders towards a commensurate magnet and this is also be a good test for powder diffraction experiments on HEIMDAL. Early neutron powder experiments on Chromium incorrectly ascribed the magnetic structure to be commensurate, due to the weak scattering and poor resolution available at that time. Powder experiments on Heimdal should be straight forward optimising the flux and resolution of the instrument. The weak magnetic scattering from the small magnetic moments will also be a good test of background from sample environment using the collimator.

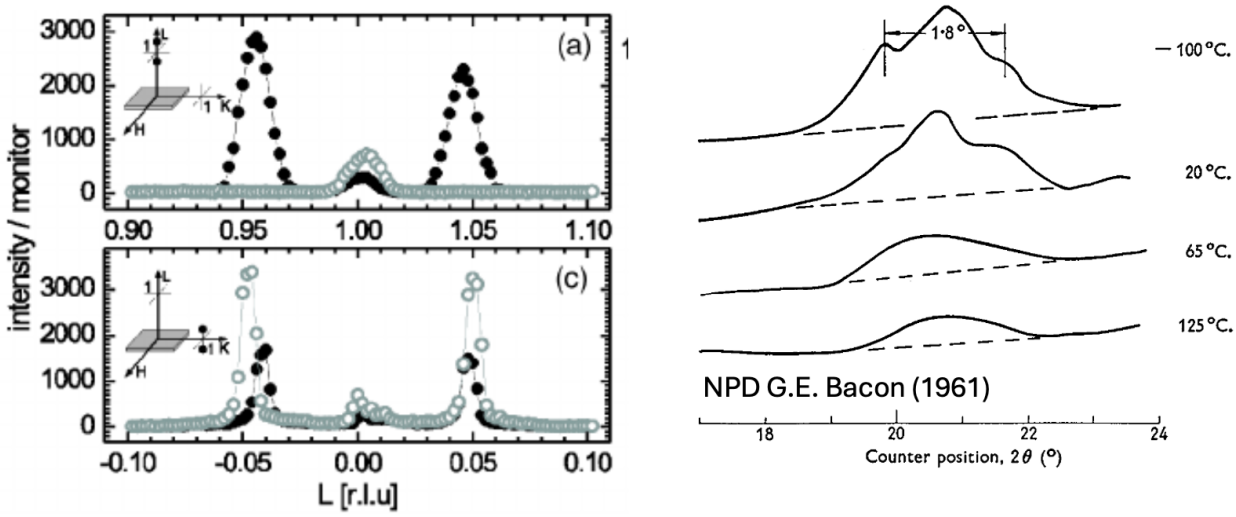

Figure 7. Diffraction neutron (left) SDW data and NPD data of the Cr SDW from 1961 (right)

4.3.3. $TmNi_2B_2C$

The rare-earth Nickel borocarbides are well known materials with both antiferromagnetic and superconducting at low temperatures. $TmNi_2B_2C$ forms a long periodic spin density wave below T_N=1.5K. This experiment will be a good test of the dilution fridge and a high resolution set-up is required to resolved the SDW satellite peaks from the nuclear peaks as shown in Figure 8. The experiment on HEIMDAL will require the use of a dilution fridge and will be a good test to characterize the background.

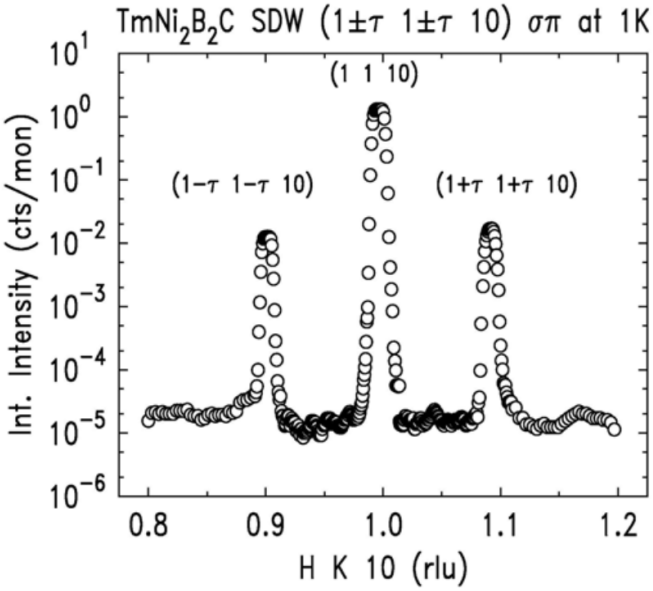

Figure 8. HK scan over the (1 1 10) Bragg peak showing the SWD in TmNi2B2C at 1.0K.

4.3.4. Holmium Metal single crystal

There could be several reasons why Holmium would make a good standard sample test case for Heimdal hot commissioning. Probably the coolest would be that the element is named after Stockholm. Secondly the element forms complex spin spiral magnetic structures, with incommensurate to commensurate transitions, conical ferromagnetic transition and spin-slip phases requiring good resolution to resolve. The material has a large magnetic moment of 10.6μ_B which will give rise to strong magnetic scattering. We have a large single crystal of Ho to test on Heimdal as shown in the figure below. The test will involve refining the complex and well-known magnetic structures as a function of temperature and determining the minimum counting time for measure a Bragg peaks towards potential single (or several) pulse magnetic scattering experiments at ESS.

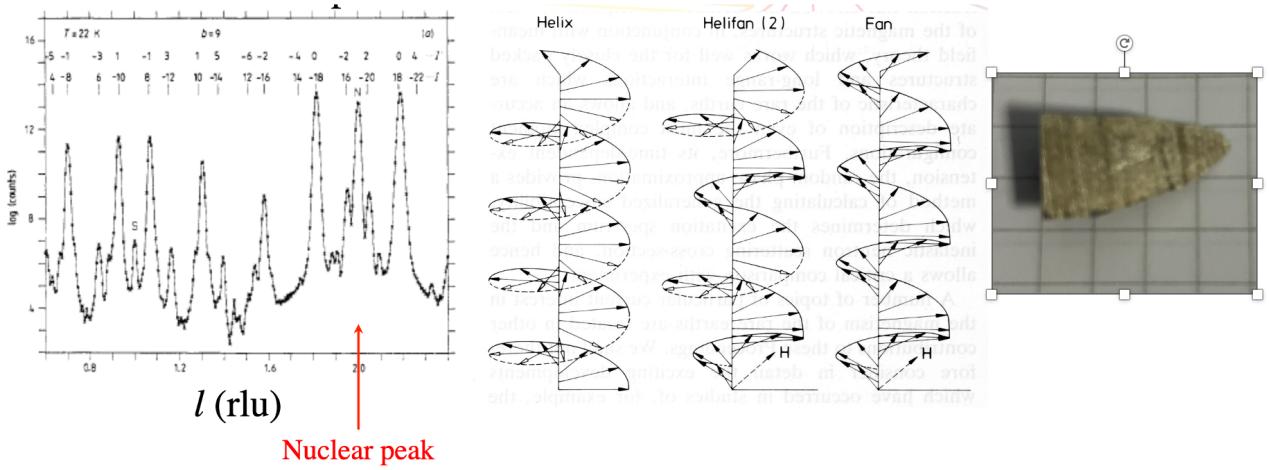

Figure 9. (Left) Neutron diffraction from Holmium showing the large number of magnetic reflections from the spin spiral structure. (Middle) The known Holmium magnetic structure. (Right) The large sample single crystal Holmium (~1.5x1.0cm) that can be used for this study.

4.3.5.Spin Caloritronic Materials

Spin caloritronic are of science interest due to their potential in next generation spintronics applications. These materials exhibit both thermoelectric and spintronic functionalities which are believed to be mediated by low energy magnon bands. Rare-earth iron garnet compound are of potential interest due to their long magnon lifetimes. The details of the magnetic structure are of importance to optimising spin caloritronic device structure. We have recently revisited the magnetic structure of $Tb_3Fe_5O_{12}$ using neutron diffraction at the D23 diffractometer at the ILL. We have been able to refine a more detailed magnetic structure that previous powder neutron experiments. Therefore, experiments using powder and single crystal $Tb_3Fe_5O_{12}$ and comparing the magnetic structure refinement will make an excellent bench marking experiment on HEIMDAL. Previous powder neutron experiments $Tb_3Fe_5O_{12}$ have failed to observe (200) and (222) type reflections as shown by the red arrows in **Error! Reference source not found.**. However, we find that these peaks are present, which allows us to refine a new structure for the double umbrella magnetic structure shown in top right of Figure 10. These peaks could not be resolved above the signal to background in the previous powder experiments. New NPD experiments will be a great test of the signal to background obtainable of HEIMDAL. Also resolving the experiments in single crystal experiments will be a good benchmark test to compare the refinements taken from the ILL experiment. $Tb_3Fe_5O_{12}$ orders into a ferrimagnetic structure at fairly temperature T_c=564K and with low temperature

rhombohedral distortion making the material an excellent case to commission the cryofurnace on HEIMDAL to make measurements in the paramagnetic phase. This is also be useful to test the background suppression using the collimator system and exploring the background level obtainable on Heimdal.

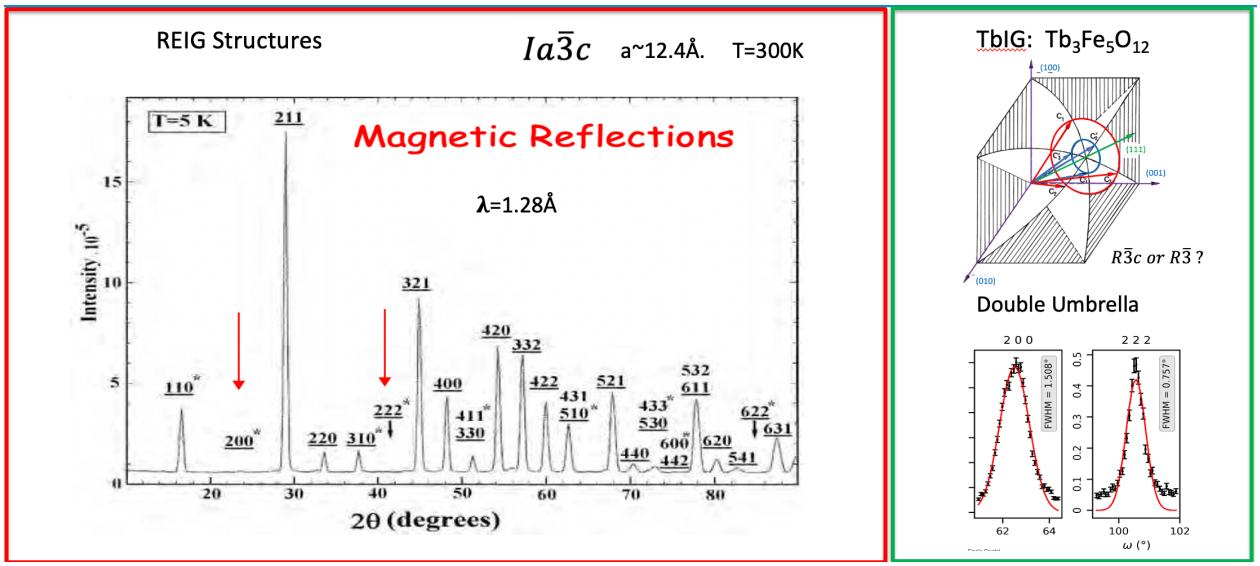

Figure 10. PND (left) data from Tb3Fe5O12 showing the absence of (200) and (222) peaks. (right) single crystal neutron diffraction showing these peaks are present.

We have made some McSTAS simulations of the expected powder and single crystal diffraction patters expected unto the HEIMDAL detector shown in figure 11 (left). The 2D detector has a fixed coverage of angles between 10-90°, as shown in Figure 11 (Right). We have tried a structural refinement of Tb3Fe5O12 using the Bragg peaks in this range from the data taken on D23 at the ILL and we still find a good refinement of these data. Therefore, the garnets represent a good case study for benchmarking experiments on HEIMDAL, largely owed to their fairly large unit cell a~12.4 Å.

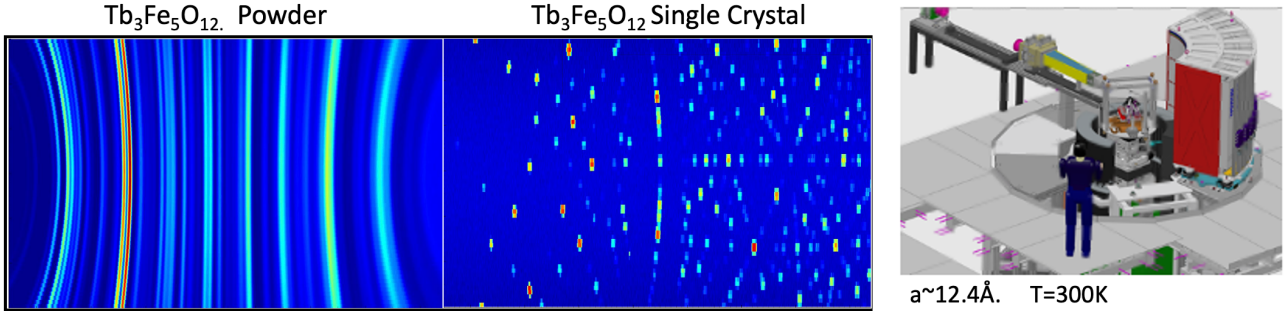

Figure 11. (Left). McSTAS simulated diffraction patterns of Tb3Fe5O12 powder and single crystals expected on the HEIMDAL detector. (Right). The reduced detector coverage on HEIMDAL.

4.3.6. Frustrated Magnets

$Tb_3Ga_5O_{12}$ is a fascinating system for complex magnetism in rare-earth quantum materials, owing to the crystal-field anisotropies, the hyperkagome sublattices, and the large dipoles and multipoles competing with exchange and hyperfine fields. Neutron diffraction has shown that TGG orders as a multiaxial antiferromagnet in zero field, with Tb^{3+} on the hyperkagome sublattices and their moments aligned along the ⟨100⟩ directions at very low temperature, T_N = 0.25 K. Recently, we have measured the magnetic structure under applied magnetic fields up to 6-Tesla along the (111) direction. The subsequent structural refinement has showed that a double umbrella is formed similar to the spin caloritronic compound $Tb_3Fe_5O_{12}$. This system would therefore make a good benchmarking experiment commissioning the cryomagnet with dilution insert on HEIMDAL, characterising the background level and to ultimately test if a similar structural refinement can be made similar to the experiment on D23 of ILL. The fact the system is a garnet with fairly large lattice parameter is also well suited to the limited detector coverage on HEIMDAL.

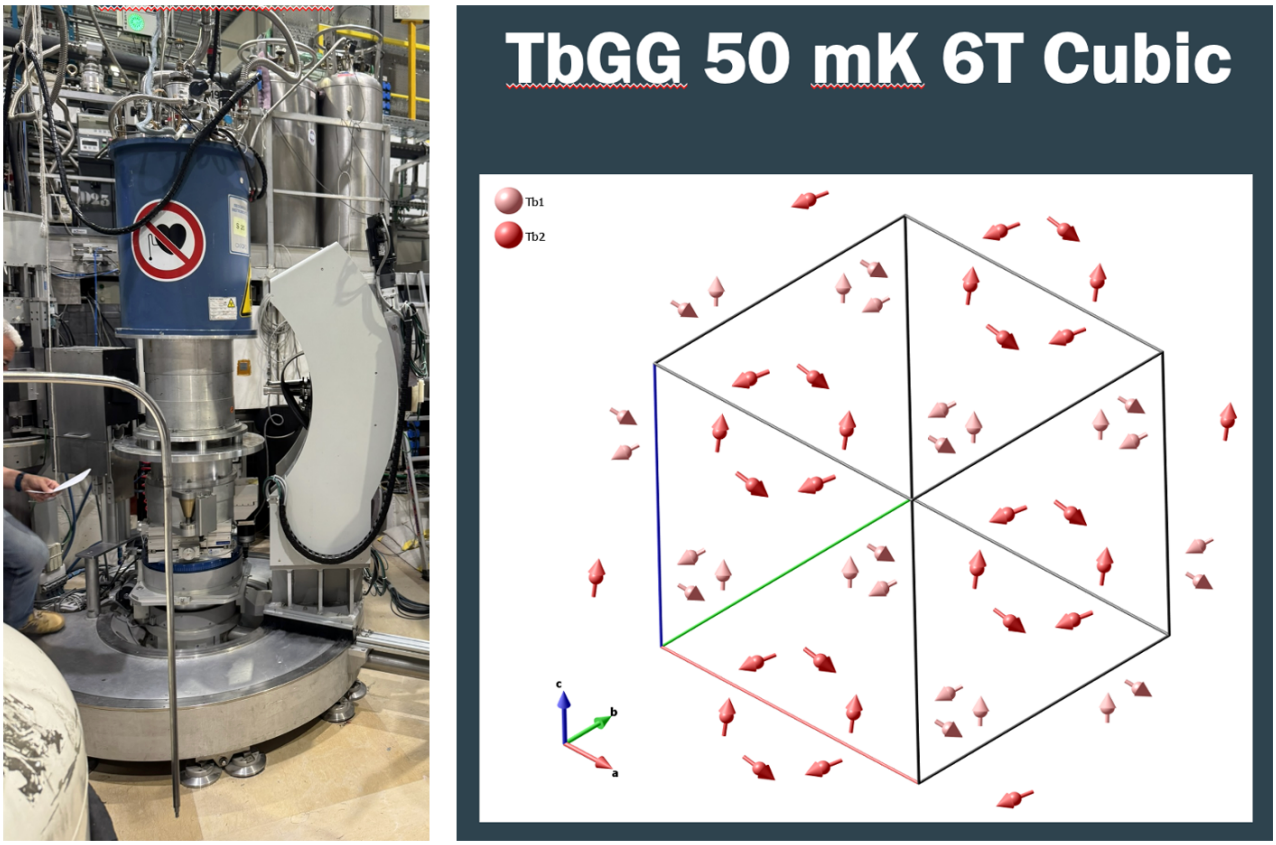

Figure. 12 (Left) The Crymagnet with dilution insert on D23 of ILL. (right) The refined magnetic structure of Tb3Ga5O12 in applied magnetic field similar to the double umbrella magnetic structure.

4.3.7.Fast Reaction time resolved experiment on Magnetic composites

One of the science cases for the instrument would focus on the high flux to follow reactions in real time in situ. One such system is based on the reduction of Fe_2O_3 to Fe_4O_4 as shown in Figure 13. Other systems could also be studies using fast induction heaters.

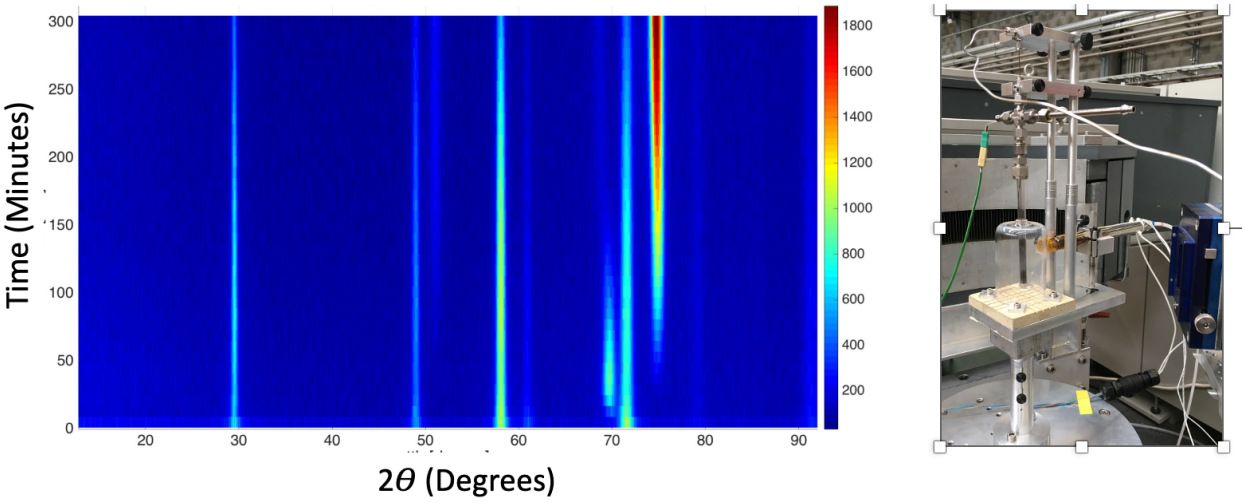

Figure 13. (left) Neutron powder diffraction date following the reduction of Fe2O3 in time. (right) The sample environment used for these experiments.

4.3.8.Thin Epitaxial Films for device applications

Many real life device applications exploit nanoscale thickness epitaxial thin films, where stain can be used to tune physical parameters. The ability to use neutron scattering to investigate these thin films would make neutron scattering of great interest to new technological industries. Recently that have been several publications exploiting neutron scattering to investigate thin film materials as shown in Figure 14. The studies are not so easy due to the very small sample volume 5x5mm x50nm and small signals. However, since the ESS will eventually be the worlds brightest source of neutrons these experiment on technologically relevant materials could become a large part of the ESS science case in the future. Here we will investigate the flux and background possibilities to investigate thin films of BiFeO3 and Tb3Fe5O12 on Heimdal. These experiments will tests the limits of HEIMDAL in terms of diffraction.

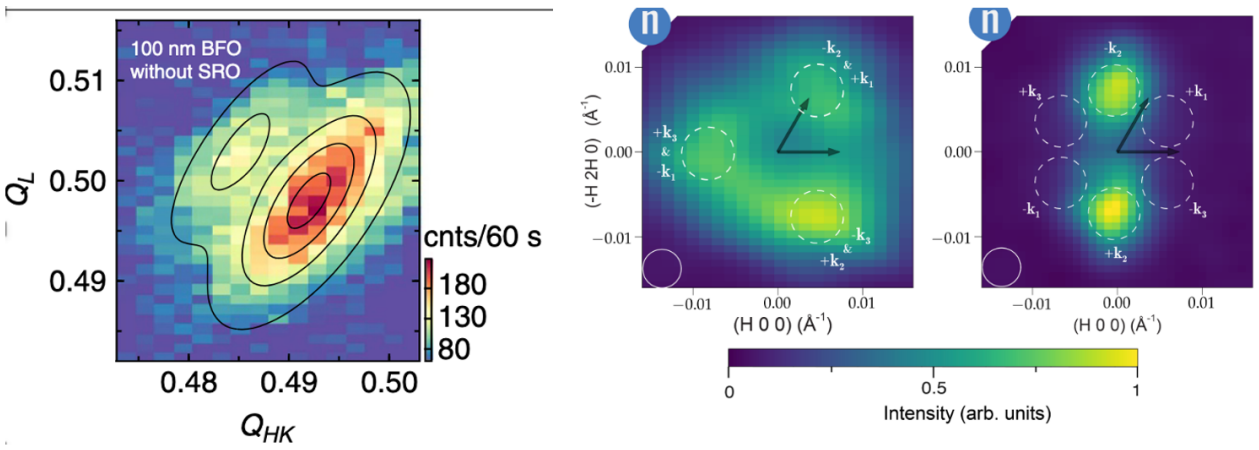

Figure 14. Left Neutron diffraction data from a BiFeO3 thin film taken at ANSTO. (Right) A Neutron diffraction from a thin film taken at WISH at ISIS.

4.4. Phase 4: Early Science Experiments.

A preliminary meeting on fist science was organised in spring of 2026, between ESS and the Heimdal in-kind partners to discuss internal ideas on first science projects, with a view that these ideas will be expanded to include external ideas during a first science diffraction workshop during the ESS/ILL user meeting in Lund in November 2026. We requested a short abstract on potential ideas in order to be able to make an analysis on feasibility, schedule and eventual science impact of the projects. At present only a few abstracts have been received but I will also give a brief overview on the expressions of interest from in-kind partners.

4.4.1. European Spallation Source (Sweden).

Dan Mannix, Neutron diffraction studies of the magnetism of spin caloritronic compounds.
Sample Environments: Cryostat, Cryofurnace, Dilution, Cryomagnet.

4.4.2. IFE (Norway)

Stefano Detedda: Neutron Powder Diffraction of Hydirdes: Hydrogen Storage
Sample Environment: Hydrogen gas in-situ (permission required from safety)

Oystein Fjellvag: Neutron Powder Diffraction Fluoroperovkites Cu(II) Cr(II) NH4CrF3
Sample Environment: Cryostat.

4.4.3. Aarhus University (Denmark)

Henrik Birkedal Neutron Powder diffraction from biominerals.
Sample Environment: Ambient conditions

Martin Bromholm Neutron single crystal Diffraction magnetic materials
Sample Environment High pressure PE Cell.

Dorthe Ravnsbaek Neutron Powder Diffraction Battery materials
Sample Environment: Battery Cells ESS and/or AU.

Shuai Wei Neutron Diffraction from liquid phase of Ge15Te85.
Sample Environment: High temperature Furnace.

Aalborg University (Denmark)
Mogens Christensen Neutron Diffraction Fe16N2.
Sample Environment: Ar+5%H_2 Gas Cell + 400K furnace.

PSI (Switzerland): No-one responded to date.

École Polytechnique Fédérale de Lausanne (Switzerland)
Livia Bove Neutron Diffraction studies of phases of ice under pressure
Sample Environment: PE cell and PE cell + hydrogen.

4.4.4.Abstracts Received So Far.

Neutron Diffraction from prototype spin caloritronic compound $Tb_3Fe_5O_{12}$

D. Mannix[1], S. Geprägs[2] T. Ziman[3] J.T. Hunt[4]
[1.]ESS, Lund Sweden, [2] WMI Munich Germany, [3]ILL, Grenoble, France, [4]Aarhus University Denmark

Background: Today, spin caloritronics are renowned for their potential in next generation spintronic devices, combining both logic and thermoelectric functionalities. $Tb_3Fe_5O_{12}$ (TbIG) is considered a prototype system for this class of materials. TbIG was proposed to have a non-collinear magnetic structure from powder neutron diffraction 40 years ago [1] (Fig.1). However, new single crystal study identify new weaker magnetic peaks not observed above background in the original powder studies, that necessitate a more complete description of TbIG structure (Fig.2). We propose to investigate powder and single crystal TbIG on Heimdal.

Commissioning/Benchmarking: The experiment will determine the signal to noise level of Heimdal with orange cryostat and collimator configuration. With observation of (200) and (222) peaks not observed in NPD. Tuning to high resolution mode will follow the T-dep rhombohedral distortion (Fig 2).

Publication/: Results will be included in our publication [2].

References:

[1] M. Lahoubi et al. IEEE Vol. Mag.20 5 p1518 (1984).
[2] J.T. Hunt et al. In preparation.

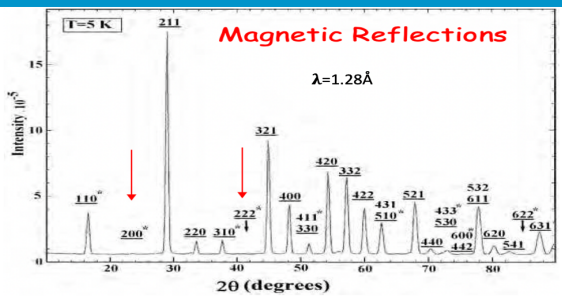

Fig.1. NPD from TbIG [1], refined with absence of (002) & (222) .

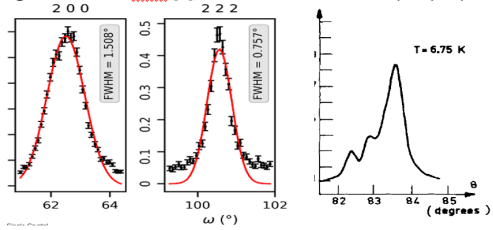

Fig.2. ND from TbIG single crystal, showing presence of (200) & (222). Also distortion (left) at 6.75K.

Mangetic and nucelar structure of NH4CrF3

Øystein S. Fjellvåg[1], Bruno Gonano[2]

[1] Department for Hydrogen Technology, Institute for Energy Technology, Kjeller NO-2027, Norway
[2] Chemistry Department and Center for Material Science and Nanotechnology, University of Oslo, Oslo NO-0315, Norway

Background Hydrogen-containing materials pose a significant challenge for neutron powder diffraction due to the strong incoherent scattering cross section of hydrogen. The Jahn–Teller active fluoroperovskite NH4CrF3 is an ideal benchmark compound for HEIMDAL, as it combines (i) ordered ammonium groups with well-defined H positions, and (ii) antiferromagnetic ordering detected by neutron diffraction. Previous neutron powder diffraction studies resolved an ammonium order–disorder transition at 405 K, subtle buckling of Cr–F–Cr bonds driven by hydrogen bonding, and magnetic reflections below the Néel temperature of 60 K, despite a strongly sloped background from incoherent hydrogen scattering [1] (Fig. 1).

Commissioning / Benchmarking We propose neutron powder diffraction measurements of NH4CrF3 on HEIMDAL to benchmark instrument performance for hydrogen-rich samples. The experiment will quantify the signal-to-background ratio arising from incoherent H scattering using standard sample environment and different collimator configurations. The dataset will serve as a reference for assessing background suppression, magnetic sensitivity, and performance limits for hydrogen-containing materials.

Publication The results will be used as a reference dataset for HEIMDAL early science and incorporated into follow-up methodological and scientific publications.

References

[1] Ø. S. Fjellvåg et al., Inorg. Chem. 63, 10594–10602 (2024).

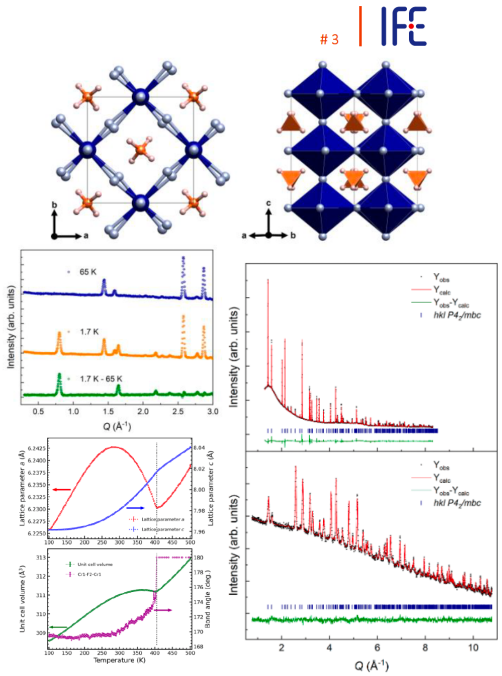

Temperature dependent neutron diffraction for fragile-strong liquid transition in Ge15Te85

Shuai Wei, Department of Chemistry, Aarhus University, Denmark.

Background: On approaching the glass transition, some liquids exhibit a near-Arrhenius rise in viscosity, while others show a range of non-Arrhenius behavior. The former is classified as "strong" liquids, while the latter is labeled as "fragile" liquids. However, some anomalous liquids, such as water or Ge-Te alloys with fundamental and application importance, do not fall into that scheme, exhibiting a fragile-strong transition (FST) associated with thermodynamic anomalies(*1*). The evolution of relaxation dynamics during the FST still remain elusive. We investigated the relaxation dynamics of $Ge_{15}Te_{85}$ at high temperature using quasi-elastic neutron scattering (QENS) with FOCUS, SINQ of PSI. The extracted QENS contributions demonstrated the emergence of the slow dynamics observed in the region of the FST, possibly suggesting the formation of the "cage" in the material. Here we propose to perform neutron diffractions near the FST to understand how structural changes are related to the dynamics from our QENS results.

Commissioning: We will collect the temperature dependent diffraction pattern from 850 K to 300 K at *Heimdal* for liquid Ge15Te85 near its FST. The results will be compared to our QENS data to understand the structure-dynamics relationships near the transition regime.

Publication: Results may be included in our publication on the liquid dynamics studies using QENs (2).

References:

1. S. Wei, P. Lucas, C. A. Angell, Phase change alloy viscosities down to Tg using Adam-Gibbs-equation fittings to excess entropy data: A fragile-to-strong transition. *J. Appl. Phys.* **118**, 034903 (2015).

2. Fujita et al. Publication under preparation (2026)

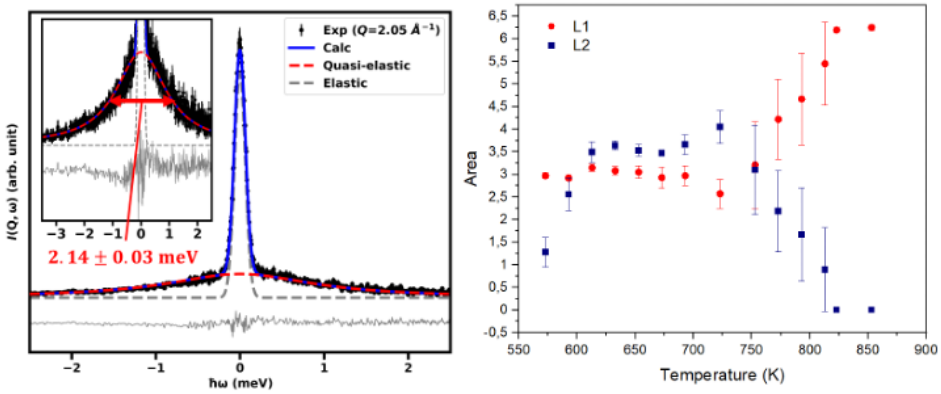

Figure 1: (left) QENS spectra of Ge15Te85 at 823 K measured on FOCUS (λ = 4.4 Å). The QENS contribution was extracted by fitting the data with a single Lorentzian. Observed data (black dots), elastic contribution (gray line), QENS contribution (red line) and the sum of calculated profiles (blue line). The full-width of half maximum of the Lorentzian profile was 2.14±0.03 meV, providing the relaxation time of 0.67±0.12 ps. It demonstrated the sub-picoseconds scale dynamics in the fragile regime. (right) Temperature dependence of the peak area of Lorentzian profiles. The model with two Lorentzians provided the best description of the QENS profile below 823 K. The contributions of the second Lorentzian (L2) stabilized below 723 K. A kink around 750 K indicates the signature of dynamic crossover. (Fujita et al. Publication under preparation (2026))

Operando neutron diffraction study of commercial lithium-ion batteries

S. Y. Lai, D. S. Wragg

Battery Technology Department, Institute for Energy Technology, Kjeller, Norway

Background: To serve ever-increasing performance demands, battery cell producers are turning to composite anode and cathode materials. Prior work performed at IFE and PSI evaluated the lithiation behavior of graphite anodes and a composite of different transition metal oxide cathode materials from a commercial ICR 10440 battery [1]. *Operando* neutron powder diffraction was performed at the HRPT diffractometer at PSI. Newer iterations of battery cells include a small amount of high capacity Si in the anode, whose lithiation potential and expansion behavior deviates strongly from those of graphite. The composite nature of a Si-graphite anode presents a complex behavior of de-/lithiation, some of which is hidden in the electroanalytical techniques due to overlap in the active voltage range. Although Si becomes amorphous with lithiation, its volume expansion has a measurable chemical and physical effect on the neighboring graphite in a coin-sized electrode [2].

Commissioning/Benchmarking: A commercial battery cell similar to that used in the prior study will be measured in *operando* neutron diffraction to establish a comparable benchmark. As a further research study, a commercial battery cell containing a Si-graphite anode will be purchased and examined using *operando* neutron diffraction.

Publication plan: Results are planned to be communicated in a communication/short publication.

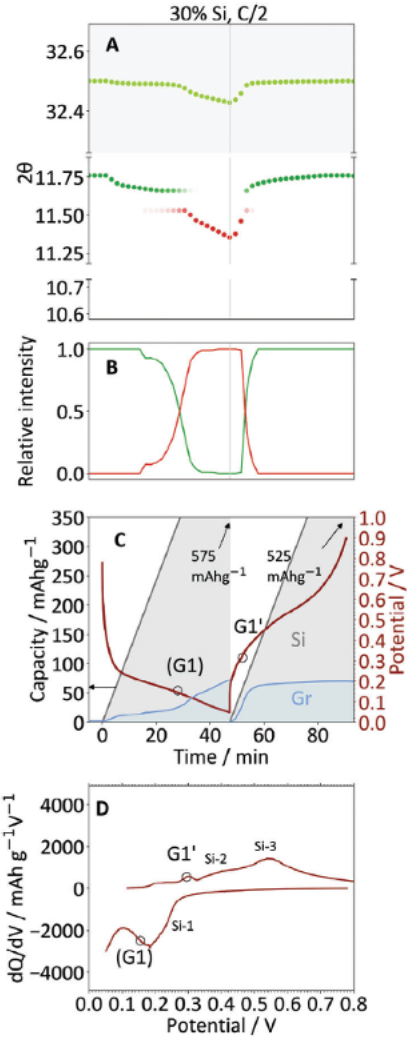

Figure 1. A study of 30% Si-Gr electrode in operando XRD and with electroanalytical techniques to determine the share of lithiation in each of graphite and Si phases.

References:

[1] N. S. Nazer, V. A. Yartys, T. Azib, M. Latroche, F. Cuevas, S. Forseth, P. J. S. Vie, R. V. Denys, M. H. Sørby, B. C. Hauback, L. Arnberg, P. F. Henry, *J. Power Sources* **2016**, *326*, 93–103.

[2] P. Schweigart, W. Hua, P. A. Sánchez, C. Lian, I.-E. Nylund, D. Wragg, S. Y. Lai, F. Cova, A. M. Svensson, M. V. Blanco, *Small* **2025**, *21*, 2406615.

DOCUMENT REVISION HISTORY

Revision	Reason for and description of change	Author	Date
1	First issue	Dan Mannix	2026-04-10